



Mutation probability-based lion algorithm for design and optimization of microstrip patch antenna

Ramakrishna Guttula¹ · Venkateswara Rao Nandanavanam²

Received: 9 March 2019 / Revised: 29 August 2019 / Accepted: 10 September 2019 / Published online: 27 September 2019
© Springer-Verlag GmbH Germany, part of Springer Nature 2019

Abstract

The advantages and performance of microstrip patch antennas (MPA) namely, reduced weight, reduced profile, and reduced cost formulate them the ideal choice for communication networks. However, the difficulties in structure size and design remain a major concern. Hence, this paper aims to propose a new model that derives a nonlinear objective model for helping in the design of solution space of antenna parameters. To attain this, it is planned to incorporate the optimization concept, thereby a new mutation probability based lion algorithm (MP-LA), which is proposed for the tuning MPA constraints. The main objective model of the antenna design is to maximize the gain by optimizing the patch length, width, thickness of substrate, and value of dielectric substrate. After executing the simulation model, this paper compares the performance of proposed MP-LA-based antenna design with numerous conventional approaches namely, antenna design without optimization, artificial bee colony-based AD, genetic-based AD, firefly-based AD, particle swarm optimization-based AD and grey wolf optimization-based AD, proposed GWO-based AD and lion optimization algorithm-based AD. Moreover, the analysis is done with respect to radiation pattern, E-plane, and H-plane of proposed and conventional antenna designs. Other performance analysis on characteristics impedance, directivity, efficiency and gain of proposed and conventional models is done.

Keywords Microstrip patch antenna · Parameter optimization · Gain · Directivity · Lion algorithm · Mutation probability

Abbreviations

MPA	Microstrip patch antenna
LA	Lion algorithm
MP-LA	Mutation probability based LA
MP-LAD	MP-LA-based antenna design
WOAD	Antenna design without optimization
AAD	Artificial bee colony-based antenna design
GAD	Genetic-based AD
FAD	Firefly-based AD
PSAD	Particle swarm optimization-based AD
GWAD	Grey wolf optimization-based AD
PGWAD	Proposed GWAD
GPS	Global position satellites
WLAN's	Wireless local area networks
EM	Electromagnetic
SLL	Side lobe level

THz	Terahertz
PBG	Photonic band gap
MTM-MIS	Modified-I-shaped electromagnetic meta materials
MWPT	Microwave wireless power transmission
RMSA	Rectangular microstrip antenna

1 Introduction

An antenna is “the part of a transmitting or receiving system that is designed to radiate or receive electromagnetic waves” [1]. A MPA [2, 3] comprises of thin metallic conductor that is linked to a thin grounded dielectric substrates. Generally, the patch is composed of gold or copper (conducting material) and it could have any feasible shape. To make simpler the performance prediction and analysis, it is commonly in rectangular, square, triangular, circular, or elliptical or in certain other shapes. MPA [4–6] can be deployed for numerous wireless appliances namely, Bluetooth, Wi-Fi, WLAN. The size minimization of MPA [7] is essential in the majority of modern-day realistic appliances, like that of GPS, mobile cellular handsets, WLAN's and other forthcoming

✉ Ramakrishna Guttula
grkjosh643@gmail.com

¹ Acharya Nagarjuna University, Guntur 522510, Andhra Pradesh, India

² Bapatla Engineering College, Bapatla, India

wireless terminals. Nowadays, patch antennas hold a very important role in communication system [8]. In recent years, the requirement for compact, low profile and broadband antennas have risen considerably owing to the extensive propagation of wireless communication technology. For dealing with this necessity, the MPA [9–11] was established in numerous applications owing to its lightweight, low cost, and low profile. Nowadays, MPA [12] has obtained the interest of researchers owing to their several beneficial features. The MPA [13, 14] structures are comparatively simpler to manufacture and have turned MPA examination into a widespread research issue. Analyzation on MPA in the twenty first century intends at increasing gain, size reduction, wide bandwidth, system-level integration and multiple functionality [15, 16].

MPA's [17–19] include a high antenna quality factor and a large quality factor results in low efficiency and narrow bandwidth. The quality factor can be minimized by raising the thickness of dielectric substrate, however, the thickness raises with the rise in the fraction of entire power contributed by the source into a surface wave that is efficiently considered as an unnecessary power loss as it is eventually scattered and it further leads to degradation of antenna features [20, 21]. The other issues namely, lower power handling capability and lower gain can be prevailed over by deploying an array configuration for the components [22], which is a compilation of homogeneous antennas that are oriented to obtain greater gain and directivity similarly in an optimal direction [23–26]. Though the geometric optimization has been reported in the literature, our novelty is in optimizing the antenna dimensions for diverse operating frequency range. Moreover, the present accomplished gain can also be significantly enhanced by appropriate heuristic principle and so this paper introduces an adaptive version of advanced optimization algorithm.

The major contribution of this paper is depicted below.

1. A new model is designed that derives a nonlinear objective model for guiding the modeling of solution space of antenna parameters.
2. A new hybrid MP-LA is proposed for the tuning the MPA constraints like patch length, width, thickness of substrate, and value of dielectric substrate for optimizing the gain.
3. The performance of proposed MP-LAD is compared with numerous conventional approaches with respect to radiation pattern, E-plane, and H-plane.
4. In addition, performance analysis on characteristics impedance, directivity, efficiency and gain of proposed and conventional models is also carried out.

The overall organization of the work is as follows: Sect. 2 portrays the literature work. Section 3 describes the design

parameters considered for modeling MPA. Section 4 portrays the MPA design based on modified lion algorithm. Section 5 discusses the experimental results, and Sect. 6 concludes the paper.

2 Literature review

2.1 Related works

In 2014, Koziel et al. [1] have suggested a surrogate-dependent optimization model to deal with a number of constraints for designing process of MPA. This scheme has deployed EM simulations of designed correction and variable fidelity models. The penalty function permits to reduce SLL, and it sustains array matching at a required level. The optimized models were attained at reduced cost equivalent to a much-increased fidelity. Finally, the experimental confirmation of the developed models of MPA arrays functioning at 10 GHz was done.

In 2018, Kushwaha et al. [2] have developed a MPA design depending on the photonic crystal for THz appliances with increased gain. The adopted antenna was distinguished with homogeneous polyimide substrate on MPA and the radiation features were analyzed. Furthermore, the performance of modelled antenna was analyzed with diverse substrate heights, PBG distance, curvature radius of patch, PBG hole radius and improved bandwidth. Therefore it was deployed for recognizing the characters of materials.

In 2014, Khandelwal et al. [3] have demonstrated an equivalent circuit design for MPA with fault ground structure. Here, precise formulations were offered for the wide-band MPA and hypothetical examination was made for the developed scheme. The antenna demonstrates superior radiation features in the whole band, and it includes a gain ranging from 5 to 12.08 dBi. In E-plane and H-plane, a least amount of isolation of 15 dB and 20 dB level was attained among cross-polarization and co-polar correspondingly. The execution of the developed antenna was analyzed and the evaluated outcomes of the fabricated antenna have revealed better performance.

In 2018, Li et al. [4] have suggested a novel narrower half-power beam width MPA array loading and high radiation gain with MIS-MTM for deploying in the MWPT. Further, a comprehensive arithmetical evaluation was done and designed in a step by step model, and optimetrics process for proposed model was performed for optimizing the modeling constraints for optimal performance. In 2017, Sharma and Sharma [5] have adopted a design of MPA by means of hybrid fractal slot together with biased ground plane for wideband appliances. The measurement on ground plane length was altered for optimizing the gain and bandwidth of antenna. It was noticed that the length of ground plane

reveals most excellent outcome in terms of gain and bandwidth. The adopted antennas were fabricated and measured and the simulated outcomes of developed antennas were distinguished with analyzed results and were noticed with realistic conformity with one another.

In 2016, Prema [6] have established a scheme on a novel modelling of multiband MPA. The introduced multiband MPA could resonate at 7 distinctive frequencies among 4 GHz and 14 GHz. For achieving frequency (multiband), a rectangular slit was introduced in the ground plane of MPA. Accordingly, the performance of adopted multiband MPA was simulated and confirmed by various analyzations. In addition, the efficiency of established multiband MPA was established through the excellent effectiveness of deliberated results. In 2014, Mathur et al. [7] have introduced a novel technique for approximating the physical dimensions of a RMSA rapidly. It was dependent on the recently established conception of “Equivalence of Design” for RMSA. Moreover, a novel scaling factor constraint was introduced and portrayed. Depending on these, transformation rules were put forward. It could be exploited for approximating the RMSA modelling constraints quickly from a “known good design”.

In 2017, Yang et al. [8] have designed WPT systems that involve two MPA arrays at 5.8 GHz. On increasing the efficiency of power transmission among the two arrays, the optimized amplitudes and phases of the excitations for both receiving and transmitting antenna components could be attained. Here, when the two arrays were detached at a distance of 40 cm, the transmission efficiency attains a value of 39.4%. In addition, if the two arrays were detached at a

distance of 100 cm, the efficiency of power transmission attains a value of 46.9%.

In 2012, Boothalingam [27], have proposed the lion algorithm with the inspiration of problem solving potential of lion. The social behaviour of lion was taken in algorithmic theme to search out optimal solutions from a huge solution space. It was to resolve single as well as multi-variable cost function problems through the generation of binary structured and integer structured lion, respectively. Finally, it was implemented and tested using De-Jong’s Type-1 functions and then the results were compared against other conventional evolutionary program. Then the test results showed best performance under varying sizes of solution spaces.

2.2 Review

Table 1 reviews the conventional techniques based on the MPA systems. At first, surrogate-based optimization was introduced in [1], which attains reduced computational cost and better fidelity model. However, there are possibilities of misalignment in radiation responses. Fringing field effect was contributed in [2] that offer better gain, and it also includes higher bandwidth, but it requires consideration on the return loss. In addition, Bessel function was deployed in [3] that generate desired bandwidth, and it also enhances the reliability. However, it needs consideration on ground length. Likewise, MIS-MTM scheme was exploited in [4], which offers optimum design values, and it also obtains high efficient transmission, yet, it has to be developed for modeling high effective transmission system. Moreover, the

Table 1 Features and challenges of MPA designs using various techniques

Author [citation]	Adopted methodology	Features	Challenges
Koziel et al. [1]	Surrogate-based optimization	Reduced computational cost Better fidelity model	Possibilities of misalignment in radiation responses
Kushwaha et al. [2]	Fringing field effect	Better gain Higher bandwidth	Requires consideration on the return loss
Khandelwal et al. [3]	Bessel function	Generates desired bandwidth More reliability	Have to focus more on ground length
Li et al. [4]	MIS-MTM	High efficient transmission Optimum design values	Have to be developed for modelling high effective transmission system
Sharma and Sharma [5]	Koch-Minkowski hybrid slot	High gain Reduced return loss	Needs much contemplation on the ground pane length
Prema [6]	Insert fed method	Attains optimal bandwidth Better accuracy	Needs contemplation on various other band applications
Mathur et al. [7]	Transformation law	Minimal error Simpler to exploit	Requires consideration on the individual values of MSA
Yang et al. [8]	WPT optimization model	Improved transmission efficiency Better bandwidth	Have to focus more on the configuration
Boothalingam [27]	Lion algorithm	Search capability is high Selection potential is simpler	Needs improvement in convergence and mutation probability rate Higher computational complexity

Koch–Minkowski hybrid Slot model was used in [5], which offers enhanced gain, and it includes reduced return loss; however, it needs much contemplation on the ground plane length. Insert fed method was exploited in [6] that provide optimal bandwidth, and it includes better accuracy, but, it has to consider more on various other band applications. Transformation law was implemented in [7], which offers minimal error and it is also simpler to exploit, yet it requires consideration on the individual values of MSA. WPT optimization model was also suggested in [8] that offers improved transmission efficiency and it also includes better bandwidth. In order to experience better search and selection, in any under estimative circumstance lion algorithm is suggested in [28], but it suffer from setback like computation, convergence and mutation probability. However, it has to focus more on configuration. Therefore, these limitations have to be considered for improving the designing of MPA effectively in the current research work.

3 Design parameters considered for modeling microstrip patch antenna

The radiation mechanism for MPA is shown in Fig. 1. The simple patch antenna includes a controlling patch and the ground plane. In the middle of this framework, a dielectric medium termed as substrate is there that has the precise value known as dielectric constant. Generally, when distinguished with the substrate and ground, the patch size is considered to be small. On modeling a MPA, a dielectric medium and resonant frequency is selected, in which the antenna has to be designed. Therefore, the values of resonant frequency and dielectric constant are based on the whole

dimensions of MPA. Moreover, a dielectric substrate with reduced dielectric constant is reasonable for improving the antenna performance, where the proficiency is enhanced with increased bandwidth and improved radiation.

It is essential to take into account of various significant constraints when modelling the MPA that is portrayed below.

Width calculation The width of MPA is depicted by Eq. (1), where, SC_p indicates the speed of light, ϵ_r signifies the dielectric substrate value and f^{res} refers to the resonant frequency. Equation (2) reveals the formulation for f^{res} , in which PL_p denotes the patch length and ϵ^{reff} refers to the effectual refractive index.

$$Wi_p = \frac{SC_p}{2f^{res}} \sqrt{\frac{2}{\epsilon_r + 1}} \tag{1}$$

$$f^{res} = \frac{SC_p}{2PL_p \sqrt{\epsilon^{reff}}} \tag{2}$$

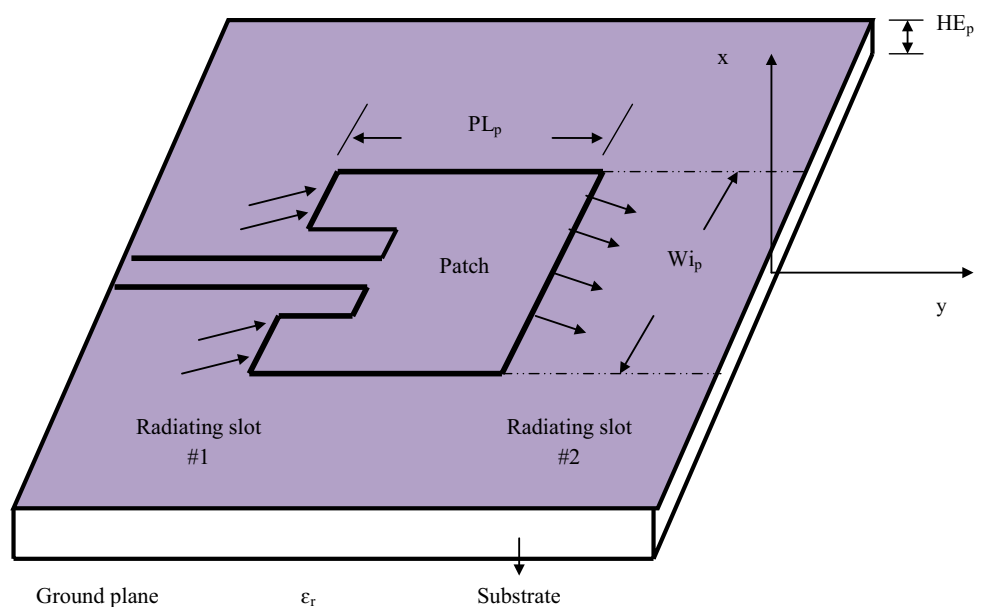
Height evaluation The height parameter HE_p is evaluated by means of Eq. (3), in which T denotes the substrate’s thickness.

$$HE_p = \frac{T}{1000 \times 2.54} \tag{3}$$

Effective refractive index calculation The parameter, ϵ^{reff} is computed by means of Eq. (4), in which HE_p denotes the height of the substrate.

$$\epsilon^{reff} = \frac{\epsilon_r + 1}{2} + \frac{\epsilon_r + 1}{2} \left[1 + 12 \frac{HE_p}{Wi_p} \right]^{-1/2}, \frac{Wi_p}{HE_p} > 1 \tag{4}$$

Fig. 1 Radiation mechanism for MPA model



Normalized length evaluation The normalized length of the MPA is denoted by ΔPL_p , which is computed as per Eq. (5).

$$\frac{\Delta PL_p}{HE_p} = 0.412 \frac{(\epsilon^{reff} + 0.3) \left(\frac{Wi_p}{HE_p} + 0.264 \right)}{(\epsilon^{reff} - 0.258) \left(\frac{Wi_p}{HE_p} + 0.8 \right)} \tag{5}$$

Length evaluation The length of the rectangular MPA, PL_p is calculated as given by Eq. (6).

$$PL_p = \frac{SC_p}{2f_{res} \sqrt{\epsilon^{reff}}} - 2\Delta PL \tag{6}$$

Characteristic impedance calculation Equation (7) shows the characteristic impedance of the transition part, in which Z_i denotes the patch impedance as exposed by Eq. (8).

$$Z_l = \sqrt{50 + Z_i} \tag{7}$$

$$Z_i = 90 \frac{\epsilon_r^2}{\epsilon_r - 1} \left(\frac{PL_p}{Wi_p} \right)^2 \tag{8}$$

Gain calculation The ratio of intensity of antenna to its input power is known as the gain of MPA. Actually, a clear antenna design offers the intensity, which is uniformly radiated in the entire directions, and does not cause any form of losses. Equation (9) indicates the gain of the MPA since the radiation intensity from a lossless isotropic antenna is equivalent to the power in antenna split by a solid angle of 4π steradians. In Eq. (9), P_{in} specifies the antenna’s input power and R_l refers to the radiation intensity

$$G_A = 4\pi \left(\frac{R_l}{P_{in}} \right). \tag{9}$$

4 Microstrip patch antenna design based on modified lion algorithm

4.1 Objective model

The objective functions of the presented MP-LA-based MPA design is to maximize the gain of patch antenna as revealed in Eq. (10). Here, the gain of the antenna is maximized by optimizing four constraints such as PL_p, Wi_p, T and ϵ_r . Thus the objective aims at enhancing the antenna gain by optimizing the above-mentioned constraints using proposed MP-LA, such that the overall MPA performance could be improved.

$$G_A^* = \arg \max_{(PL_p, Wi_p, T, \epsilon_r)} (G_A) \tag{10}$$

4.2 Solution encoding

Assume the design of MPA with constraints namely, patch length (PL_p), width (Wi_p), thickness of substrate (T) and value of dielectric substrate (ϵ_r). On modelling the antenna, it is required to increase its gain which can be attained by optimizing the above mentioned four constraints. The solution that is to be optimized is revealed in Fig. 2. The solution that involves these constraints is given to the proposed MP-LA approach for attaining maximized gain. Here, the constraints PL_p, Wi_p, T and ϵ_r are together indicated as Q , which is offered as the solution vector.

4.3 Conventional lion optimization

The LA [27] optimization is used for large-scale and standard bilinear systems. Different from other cat species, lions continue to exist with a fascinating social system/behaviour, known as pride, to make stronger their own species at all generations. Usually, a pride includes one to three lion pair where the resident females attract males to give birth to young ones. The residing region of these lions is known as territory. The dominating lion of a terrain governs the particular area by combating against other animals together with nomadic lions. The territorial defence persists till the cubs achieve sexual maturity, probably for 2–4 years. The progress of this LA model is continued with four imperative steps i.e., mating, pride generation, territorial takeover and territorial defence.

Here, the solution vector is specified by O and is indicated by $O = [o_1, o_2, \dots, o_m]$.

Pride generation The initialization of pride is made with territorial lion O^{mal} and lioness O^{fem} and a nomadic lion O^{nd} .

The vector element of O^{mal}, O^{fem} and O^{nd} is represented as $o_{len}^{mal}, o_{len}^{fem}$ and o_{len}^{nd} , which are considered as the random integers that lies in the maximum and minimum limits while $m > 1$, in which $len = 1, 2 \dots, Len$. Here, the length of lion is indicated as Len and is specified by Eq. (11), in which, n and m are integers.

$$Len = \begin{cases} m; & m > 1 \\ n; & \text{otherwise} \end{cases} \tag{11}$$

When $m = 1$, the constraints given in Eqs. (12) and (13) have to be satisfied, and $R(o_{len})$ is given by Eq. (14).



Fig. 2 Solution encoding representation

$$R(o_{len}) \in (o_{len}^{\min}, o_{len}^{\max}) \tag{12}$$

$$n\%2 = 0 \tag{13}$$

$$R(o_{len}) = \sum_{len=1}^{Len} o_{len} 2^{\left(\frac{Len}{2} - len\right)} \tag{14}$$

Fertility evaluation The local optima or global optima is attained by the laggards when O^{fem} and O^{mal} gets saturated by the fitness. Here, the laggard is regarded as O^{mal} and the laggardness rate is specified as La_r , and is maximized by 1, when fitness of male lion $f(O^{mal})$ is higher than f^r that indicates reference fitness. After crossover, the fertility of O^{fem} is confirmed by sterility rate St_r , and is maximized by 1. When St_r becomes higher than the tolerance St_r^{\max} , then the update for O^{fem} is done as per Eq. (15). The mating process could be carried out, when the updated female O^{fem+} is considered as O^{fem} , due to its enhancement. In Eqs. (15) and (16), o_{len}^{fem+} and o_d^{fem} are considered as len^{th} and d^{th} vector element of O^{fem+} correspondingly and ∇_d is given by Eq. (17).

$$o_{len}^{fem+} = \begin{cases} o_d^{fem+} & \text{if } len = d \\ o_{len}^{fem} & \text{otherwise} \end{cases} \tag{15}$$

$$o_d^{fem+} = \min[o_d^{\max}, \max(o_d^{\min}, \nabla_d)] \tag{16}$$

$$\nabla_d = \left[o_d^{fem} + (0.1r_2 - 0.05)(o_d^{mal} - r_1 o_d^{fem}) \right] \tag{17}$$

Arbitrary integer d is produced in the limits between [1, Len], the female update operation is indicated by ∇ and the arbitrary integer is specified as r_1 and r_2 that are produced in the limits between [0, 1].

Mating Crossover and mutation are the two major steps in this process. By this, the cubs are generated by O^{mal} and O^{fem} . Thus, four cubs are produced by a lioness pregnancy and thus four cubs are generated by the crossover process.

Lion operators Territorial defence enables the approach to discover various solutions with identical fitness. If Eq. (18) to Eq. (20) are met with, then O^{e-nd} will be chosen.

$$f(O^{e-nd}) < f(O^{mal}) \tag{18}$$

$$f(O^{e-nd}) < f(O^{mal_cub}) \tag{19}$$

$$f(O^{e-nd}) < f(O^{fem_cub}) \tag{20}$$

The pride update takes place only after the defeat of O^{mal} , whereas the updation of nomad coalition takes place only after the defeat of O^{nd} . Territorial takeover forces the model to update O^{mal} and O^{fem} if O^{mal_cub} and O^{fem_cub} are matured, i.e. when the age of cubs goes beyond the highest age for cub maturity, A^{\max} .

Termination The implementation of algorithm will terminate only if any of the two conditions as given in Eqs. (21) and (22) is satisfied. In Eq. (21), iteration is specified as it which is fixed as zero initially and increased by 1 while territorial takeover is performed.

$$it > it_{\max} \tag{21}$$

$$f(Z^{mal}) - f(Z^{opt}) \leq er_{th} \tag{22}$$

The error threshold and maximum count of generations is specified by er_{th} and it_{\max} , correspondingly. The pseudo code of the conventional LA model is given by Algorithm 1

Algorithm 1: Conventional LA Model
Initialize O^{mal} , O^{fem} and O_1^{nd}
Evaluate $f(O^{mal})$, $f(O^{fem})$ and $f(O_1^{nd})$
Fix $f^r = f(O^{mal})$ and $it = 0$
Store O^{fem} and $f(O^{mal})$
Carry out fertility computation
Carry out mating and attain cub pool (crossover and mutation)
Mutation
If $rand > 0.5$
Perform mutation on female lion based on mutation rate
else
Perform mutation on male lion based on mutation rate
Carry out territorial defense; if defense result 0, go to step 4
If $A^{cub} < A^{\max}$, follow step 9.
Carry out territorial takeover and obtain updated O^{mal} and O^{fem}
Increment it by one
If the termination criteria are not met, go to step 4, otherwise terminate the process.

4.4 Proposed MP-LA algorithm

In order to improve the performance of the conventional LA, the proposed concept is developed. In the conventional LA, only the mutation rate is taken into consideration. As an improvement in conventional LA, the mutation probability, indicated by MP is considered in modified LA, by which the performance could be improved. Since the adopted modification on LA depends on a parameter called mutation probability, the proposed algorithm can be termed as MP-LA. The mutation probability MP is formulated as shown in Eq. (23), where, $f(O^{fem})$ indicates the fitness of female lion and $f(O^{mal})$ points out the fitness of male lion and C_{it} denotes the current iteration. The pseudo code of the proposed MP-LA model is given by Algorithm 2

outcomes were obtained. Here, the antenna was designed with increased efficiency and high gain by deploying the adopted MP-LA approach by considering numerous constraints namely, L_p, W_p, T and ϵ_r . Accordingly, in the presented research work, the population size was allocated as 10 and entire number of iteration was allocated as 100. Following the simulation, the performance of the adopted antenna design was evaluated with numerous conventional schemes namely, WOAD [21], AAD [29], GAD [30], FAD [31], PSAD [32], GWAD [33], PGWAD [34] and LAD [27] design models to substantiate the efficiency of the presented antenna design.

Algorithm 2: Proposed MP-LA Model
Initialize O^{mal}, O^{fem} and O_1^{nd}
Evaluate $f(O^{mal}), f(O^{fem})$ and $f(O_1^{nd})$
Fix $f^r = f(O^{mal})$ and $it = 0$
Store O^{fem} and $f(O^{mal})$
Carry out fertility computation
Carry out mating and attain cub pool (crossover and mutation)
Mutation
Determine mutation probability using Eq. (23)
If $rand > 0.5$
Perform mutation on female lion based on mutation rate and mutation probability
else
Perform mutation on male lion based on mutation rate and mutation probability
Carry out gender clustering and attain O^{mal_cub} and O^{fem_cub}
Assign A^{cub} as 0
Simulate the function of cub growth
Carry out territorial defense; if defense result 0, go to step 4
If $A^{cub} < A^{max}$, follow step 9.
Carry out territorial takeover and obtain updated O^{mal} and O^{fem}
Raise it by one
If the termination criteria are not met, go to step 4, otherwise terminate the process.

$$MP = \left(\frac{f(O^{fem})}{f(O^{mal})} \right) * \left(\frac{1}{C_{it}} \right) \tag{23}$$

5 Results and discussions

5.1 Simulation procedure

The implementation of the design of MPA using proposed MP-LAD was performed in MATLAB 2018a, and the

5.2 Performance analysis

The performance analysis of the proposed MP-LA-based MPA in terms of characteristics impedance, directivity, efficiency, and gain is given by Fig. 3. From the analysis, it could be known that the designed parameters (characteristic impedance, directivity, efficiency, and gain) of the proposed scheme are better than the conventional schemes with respect to varying frequencies. From Fig. 3a, the characteristic impedance of the presented scheme is 14% better

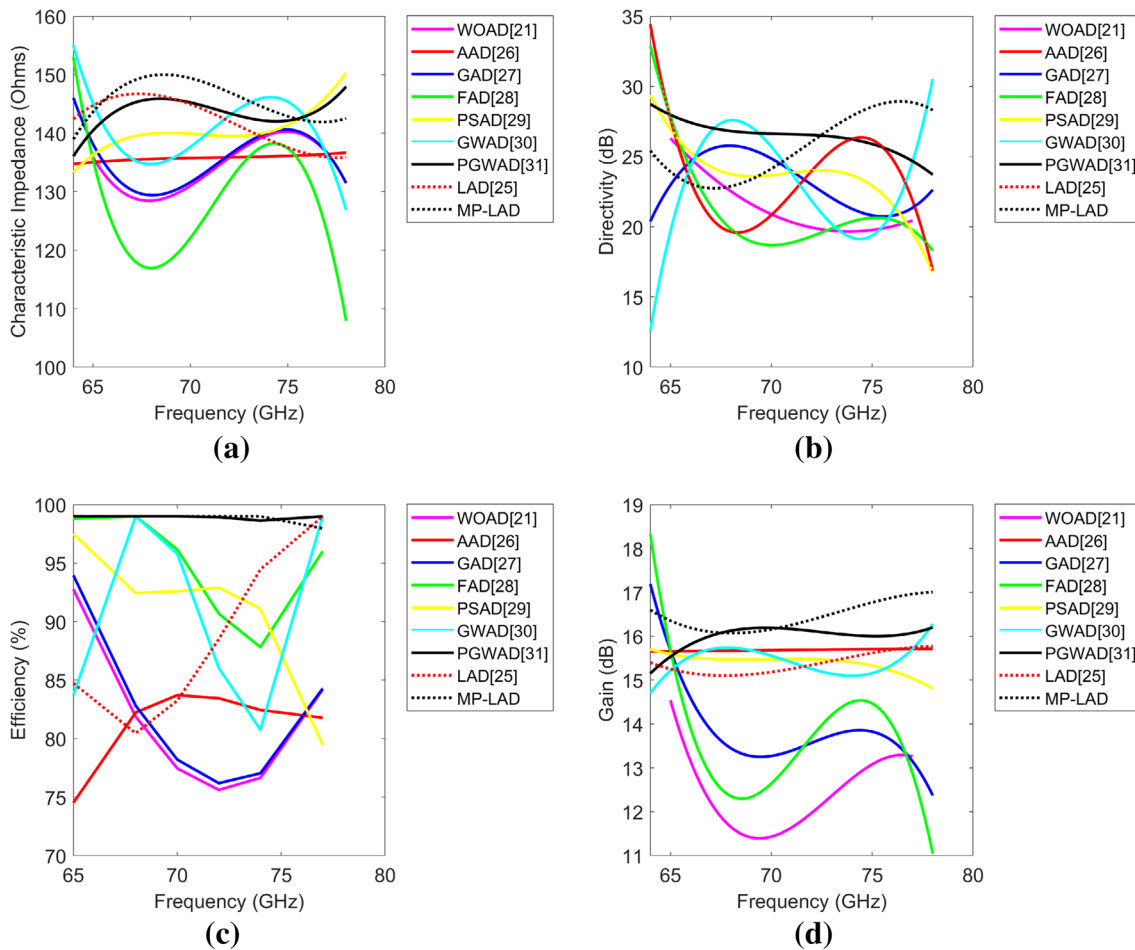


Fig. 3 Performance analysis of the proposed and traditional MPA design with respect to frequency in terms of **a** characteristic impedance **b** directivity **c** efficiency **d** gain

than WOAD, 10% better than AAD, 12.67% better than GAD, 22.67% better than FAD, 6.67% better than PSAD, 10.67% better than GWAD, 3.33% better than PGWAD and 3.33% better than LAD algorithms at 68 GHz. Likewise, from Fig. 3b, at 75 GHz, the directivity of the suggested MP-LA method is 29.82% superior to WOAD, 8.77% superior to AAD, 24.56% superior to GAD, 24.56% superior to FAD, 17.54% superior to PSAD, 33.33% superior to GWAD, 8.77% superior to PGWAD and 8.77% superior to LAD algorithms. In addition, from Fig. 4c, the efficiency of the proposed MP-LA model is 23.23% better than WOAD, 16.16% better than AAD, 22.22% better than GAD, 11.11% better than FAD, 7.07% better than PSAD, 17.17% better than GWAD, 1.01% better than PGWAD and 5.05% better than LAD algorithms at 73 GHz. From Fig. 4d, the gain of the introduced MP-LA model at 78 GHz is 22.35% superior to WOAD, 7.65% superior to AAD, 18.82% superior to GAD, 14.71% superior to FAD, 10.59% superior to PSAD, 11.76% superior to GWAD, 5.88% superior to PGWAD and 7.65% superior to LAD algorithms. In addition, the overall

performance analysis of the proposed MP-LA-based MPA is given by Table 2. From the analysis, the overall gain of the presented scheme is 30.35% superior to WOAD, 4.72% superior to AAD, 18.81% superior to GAD, 20.54% superior to FAD, 6.6% superior to PSAD, 6.46% superior to GWAD, 2.59% superior to PGWAD and 6.95% superior to LAD algorithms. Hence, better efficiency could be obtained by the adopted MP-LAD scheme when evaluated with other traditional schemes. Thus the betterment of the proposed method has been substantiated from the simulation outcomes.

5.3 Beam forming

The beam formation (radiation pattern) of adopted MP-LAD based antenna design over the traditional antenna designs is revealed in Fig. 4 from its operation at varied frequencies namely, 65 GHz, 68 GHz, 70 GHz, 72 GHz, 74 GHz, and 77 GHz. As per Fig. 4a, the radiation pattern of the implemented antenna model has attained a bigger main lobe and side lobes than the conventional designs at a frequency of

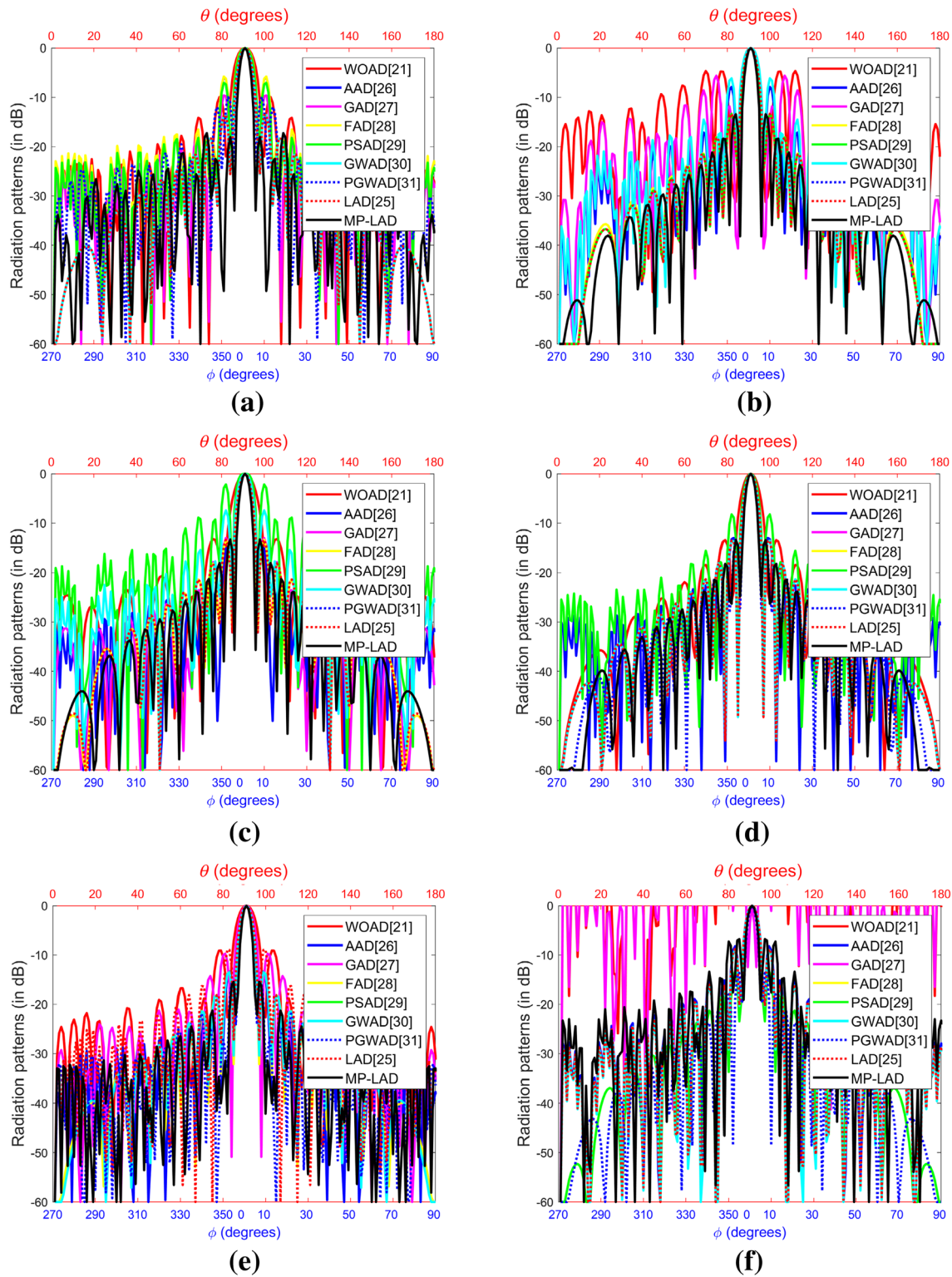


Fig. 4 Radiation pattern of proposed and traditional MPA design for various frequencies namely **a** 65 GHz, **b** 68 GHz, **c** 70 GHz, **d** 72 GHz, **e** 74 GHz and **f** 77 GHz

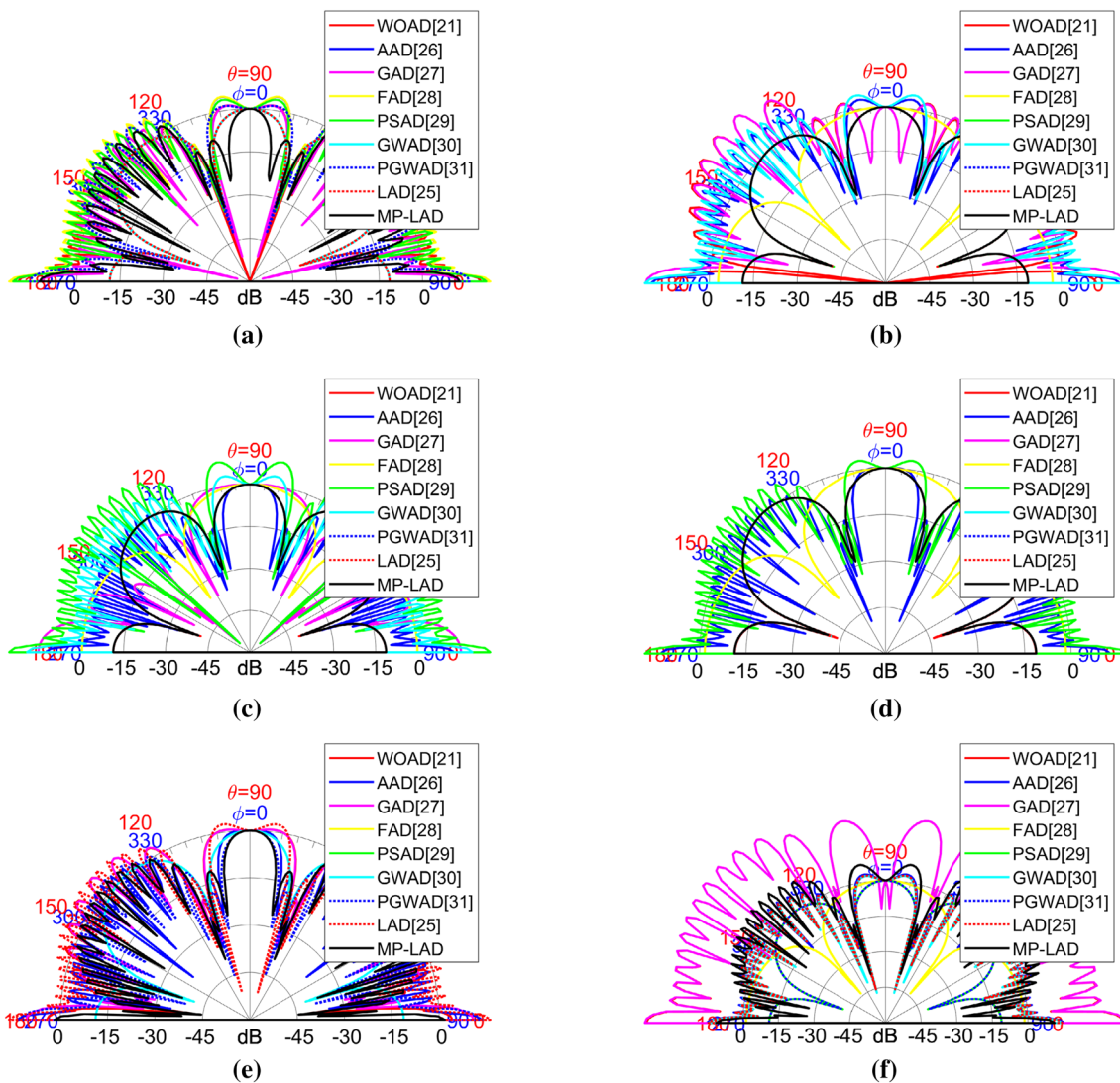
Table 2 Overall performance analysis on design constraints of proposed and conventional antenna designs

Methods	Gain	Efficiency	Directivity	Characteristic impedance
WOAD [21]	12.603	8142.8	21.629	134.59
AAD [29]	15.687	8135.7	23.38	135.78
GAD [30]	13.827	8208.5	23.207	135.39
FAD [31]	13.629	9505.7	20.974	127.99
PSAD [32]	15.411	9100.3	23.605	140.35
GWAD [33]	15.431	9129.4	23.113	140.51
PGWAD [33]	16.013	9937.8	26.477	143.64
LAD [27]	15.361	8871.9	25.625	142.19
MP-LAD	16.428	9983.8	22.33	145.99

65 GHz. From Fig. 4b, the radiation pattern of the adopted antenna model has attained a bigger size of main lobe and side lobes than the conventional designs at a frequency of 68 GHz. Likewise, from Fig. 4c, f the adopted MP-LAD scheme has attained main lobe and side lobes whose size are bigger than the other compared traditional schemes at a varying frequencies of 68 GHz, 70 GHz, 74 GHz, and 77 GHz respectively.

5.4 E plane analysis

The linearly polarized antenna consists of an E-plane that includes direction of maximum radiation and electric field vector. Generally, E-plane has the capability to find out the

**Fig. 5** E-plane of proposed and traditional MPA design for various frequencies namely **a** 65 GHz, **b** 68 GHz, **c** 70 GHz, **d** 72 GHz, **e** 74 GHz and **f** 77 GHz

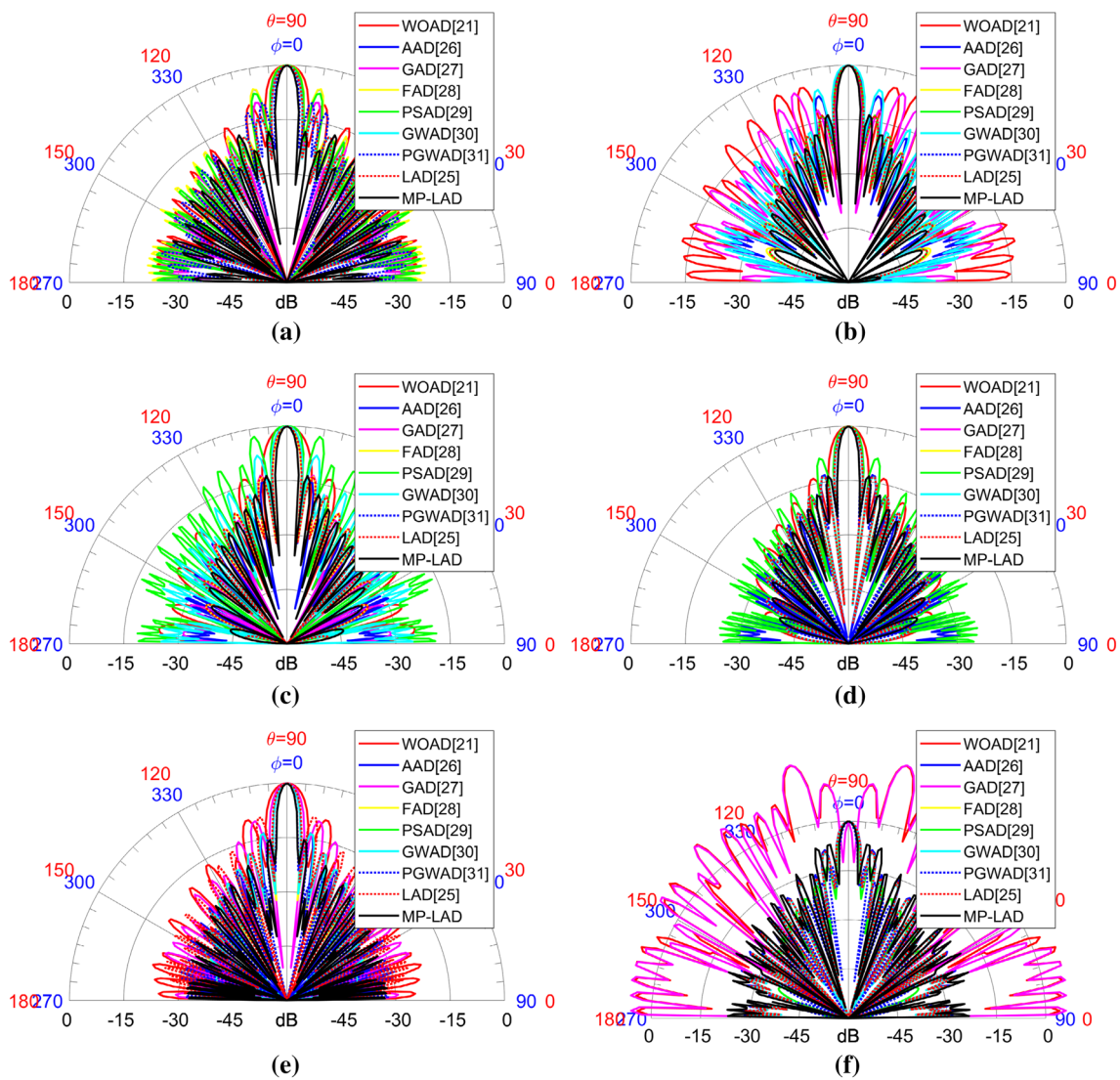


Fig. 6 H-plane of proposed and traditional MPA design for various frequencies namely **a** 65 GHz, **b** 68 GHz, **c** 70 GHz, **d** 72 GHz, **e** 74 GHz and **f** 77 GHz

polarization or orientation of radio waves of the antenna. Here, E-plane of the modelled MPA by changing the frequency at 65 GHz, 68 GHz, 70 GHz, 72 GHz, 74 GHz, and 77 GHz is revealed in Fig. 4, in which the DOA is set as 90°. The efficient antenna model is attained only if the main lobe and side lobes obtain maximum dimension. From Fig. 5a, the size of the main lobe and side lobes provided by the proposed MP-LA model is larger than the conventional WOAD, AAD, GAD, FAD, PSAD, GWAD, PGWAD, and LAD design models for the MPA model at a frequency of 65 GHz. In addition, from Fig. 4b, c the size of main lobe of adopted MP-LAD modelled antenna seems to be high and the side lobes are far bigger than the existing models at frequency 68 GHz and 70 GHz. Similarly, from Fig. 5d–f,

the size of main lobe and side lobes of MPA for the proposed scheme at varied frequencies namely, 72 GHz, 74 GHz and 77 GHz are found superior to the traditional schemes.

5.5 H plane analysis

The H-plane of MPA comprises of the direction of maximum radiation in addition to the magnetic field vector. Accordingly, the H-plane of the implemented MP-LAD scheme and conventional schemes at diverse frequencies namely, 65GHz, 68 GHz, 70 GHz, 72 GHz, 72 GHz, 74 GHz and 77 GHz is demonstrated by Fig. 6. Here, at the entire frequencies, i.e. (Fig. 6a–f) the size of the side lobe and main lobes of the presented antenna design are bigger than

Table 3 Overall performance analysis on proposed and conventional models interms of test functions

Models	Measures	AAD [29]	GAD [30]	FAD [31]	PSAD [32]	GWAD [33]	PGWAD [33]	LAD [27]	MP-LAD
Ackley	Mean	2.035	18.648	0.00402	7.6997	7.64 e ⁻¹⁵	15.843	15.843	4.44e ⁻¹⁵
	SD	0.68533	0.72954	0.000949	5.2786	1.08 e ⁻¹⁵	1.3803	1.3803	0
Dixon-Price	Mean	0.32005	11.553	0.00126	3.1323	6.81E-15	4.56 e ⁻¹⁵	7.538	8.88e ⁻¹⁶
	SD	0.26652	0.39038	0.000258	1.016	1.70 e ⁻¹⁵	6.49e ⁻¹⁶	0.92118	0
Griewank	Mean	0.41939	183.16	0.089923	3.744	0.018484	39.388	39.388	0.00057
	SD	0.15647	27.893	0.092316	7.6133	0.027574	10.975	10.975	0.00312
Levy	Mean	0.002702	8.1368	8.08E-07	2.914	0.21845	0.2625	7.6833	1.50e ⁻³²
	SD	0.002512	1.5453	7.38e ⁻⁰⁷	2.6688	0.097492	0.1429	2.7504	1.11e ⁻⁴⁷
Rastrigin	Mean	6.9483	55.518	14.526	31.184	0.39188	0	50.747	0
	SD	1.835	13.392	6.1199	13.155	0.87855	0	12.12	0
Schwefel	Mean	585.61	3716.7	1542.5	1437.4	1796.7	2078.1	1405.4	0.00018
	SD	117.29	103.95	423.26	495.67	266.1	398.07	453.77	4.75e ⁻⁰⁵
Sphere	Mean	0.00038	7.6238	2.74e ⁻⁰⁷	1.2246	1.55e ⁻⁶⁸	1.69e ⁻¹²³	8.5389	0
	SD	0.00053	4.2613	1.12E-07	2.4534	4.19e ⁻⁶⁸	9.07e ⁻¹²³	3.5134	0
Sum squares	Mean	0.00205	3.7812	1.39e ⁻⁰⁶	5.4285	2.79e ⁻⁶⁸	2.03e ⁻¹²⁴	46.772	0
	SD	0.002143	3.078	7.04e ⁻⁰⁷	10.792	1.05e ⁻⁶⁷	7.41e ⁻¹²⁴	17.017	0
Zakharov	Mean	34.54	121.43	1.80e ⁻⁰⁶	220.18	1.38 e ⁻³⁵	47.696	47.696	1.01e ⁻⁵⁷
	SD	8.9956	38.895	8.46e ⁻⁰⁷	92.698	5.64e ⁻³⁵	15.242	15.242	3.36e ⁻⁵⁷

the traditional designs. Therefore, the enhancement of the adopted MP-LAD model in terms of H-plane has been validated from the analysis.

5.6 Performance test validation

Table 3 shows the performance comparison of the proposed model over conventional model interms of various test functions like Ackley, Dixon-Price, Griewank, Levy, Rastrigin, Schwefel, Sphere, Sum Squares and Zakharov. The mean and the standard deviation of the proposed and the conventional models are calculated by computing each algorithms 30 times. The outcome proved that the proposed model shows better results when compared to that of conventional models.

5.7 Convergence analysis

The convergence of the proposed and conventional models are shown in Fig. 7. It depicts that the proposed model shows better converge rate when compared to that of conventional models in terms of varied in frequency.

5.8 S11 parameter analysis

The S parameter is examined for 65 GHz, and its frequency is illustrated in Fig. 8.

6 Conclusion

This paper has presented a new MP-LA-based design of MPA, which was based on a nonlinear objective model for the modeling of solution space of antenna parameters. The constraints like patch length, width, thickness of substrate and value of dielectric substrate was optimized by proposed MP-LA in order to attain the objective focussing maximization of gain. Further, this paper has compared the performance of adopted MP-LAD with numerous conventional approaches on considering radiation pattern, E-plane, and H-plane. In addition, analysis was done by observing characteristics impedance, directivity, efficiency and gain of proposed and conventional models. From the simulation outcomes, the effective performance of the adopted antenna design could be found which was better than the traditional models. Here, the characteristic impedance of the presented scheme was 14% better than WOAD, 10% better than AAD, 12.67% better than GAD, 22.67% better than FAD, 6.67% better than PSAD, 10.67% better than GWAD, 3.33% better than PGWAD and 3.33% better than LAD algorithms at 68 GHz. Likewise, the directivity of the suggested MP-LA method at 75 GHz was 29.82% superior to WOAD, 8.77% superior to AAD, 24.56% superior to GAD, 24.56% superior to FAD, 17.54% superior to PSAD, 33.33% superior to GWAD, 8.77% superior to PGWAD and 8.77% superior to LAD algorithms. Therefore, the efficiency of the adopted MP-LAD scheme has been verified through valuable analysis.

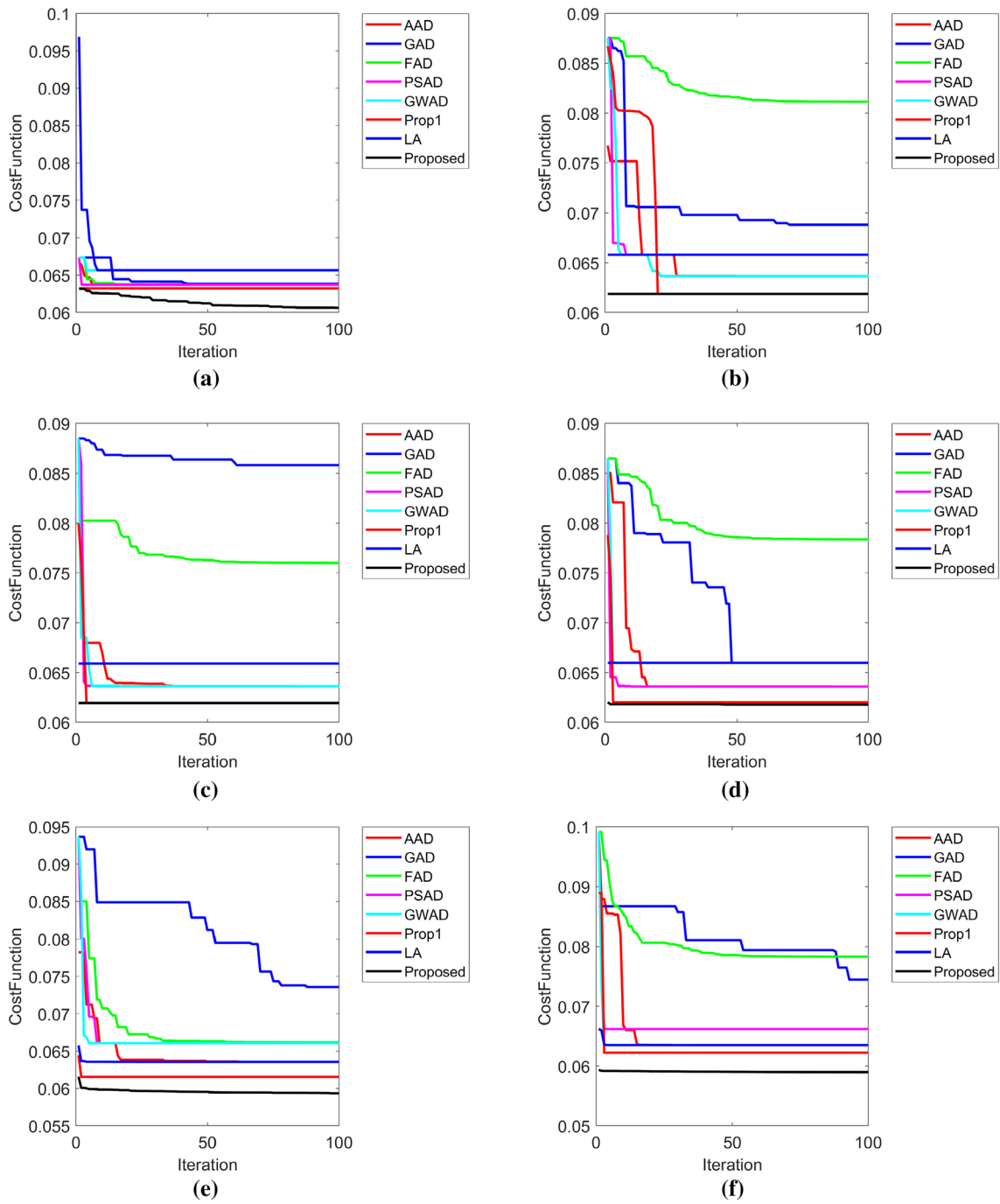


Fig. 7 Convergence of the proposed and conventional MPA design models for various frequencies namely **a** 65 GHz, **b** 68 GHz, **c** 70 GHz, **d** 72 GHz, **e** 74 GHz and **f** 77 GHz

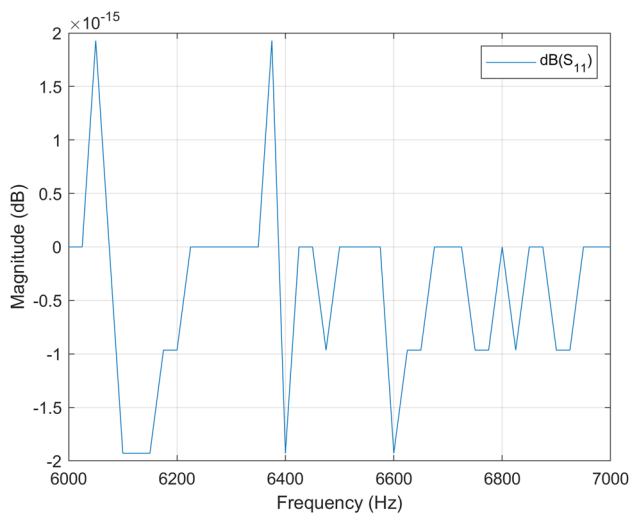


Fig. 8 S11 parameter graph for 65 GHz frequency

References

- Koziel S, Ogurtsov S, Zieniutycz W, Sorokosz L (2014) Expedited design of microstrip antenna subarrays using surrogate-based optimization. *IEEE Antennas Wirel Propag Lett* 13:635–638
- Kushwaha RK, Karuppanan P, Malviya LD (2018) Design and analysis of novel microstrip patch antenna on photonic crystal in THz. *Phys B Condens Matter* 545:107–112
- Khandelwal MK, Kanaujia BK, Dwari S, Kumar S, Gautam AK (2014) Analysis and design of wide band microstrip-line-fed antenna with defected ground structure for Ku band applications. *AEU Int J Electron Commun* 68(10):951–957
- Li TQ, Ma B, Du XF, Chen HY, Lv WR (2018) A novel design of microstrip patch antenna array with modified-I-shaped electromagnetic metamaterials applied in microwave wireless power transmission. *Optik* 173:193–205
- Sharma N, Sharma V (2017) A design of microstrip patch antenna using hybrid fractal slot for wideband applications. *Ain Shams Eng J* 9:2491–2497
- Prema N (2016) Design of multiband microstrip patch antenna for C and X band. *Optik* 127(20):8812–8818
- Mathur D, Bhatnagar SK, Sahula V (2014) Quick estimation of rectangular patch antenna dimensions based on equivalent design concept. *IEEE Antennas Wirel Propag Lett* 13:1469–1472
- Yang X, Geyi W, Sun H (2017) Optimum design of wireless power transmission system using microstrip patch antenna arrays. *IEEE Antennas Wirel Propag Lett* 16:1824–1827
- Bhongale SR, Ingavale HR, Shinde TJ, Vasambekar PN (2018) Microwave sintered Mg–Cd ferrite substrates for microstrip patch antennas in X-band. *AEU Int J Electron Commun* 96:246–251
- Saxena NK, Kumar N, Pourush PKS (2015) Radiation characteristics of microstrip rectangular patch antenna fabricated on LiTiMg ferrite substrate. *AEU Int J Electron Commun* 69(12):1741–1744
- Gupta M, Mathur V (2018) Koch boundary on the square patch microstrip antenna for ultra wideband applications. *Alex Eng J* 57(3):2113–2122
- Emadeddin A, Shad S, Rahimian Z, Hassani HR (2017) High mutual coupling reduction between microstrip patch antennas using novel structure. *AEU Int J Electron Commun* 71:152–156
- Nuangpirom P, Klinbumrung K, Tangthong N, Akatimagool S (2016) Wave iterative computation for fractal microstrip patch antenna. *Procedia Comput Sci* 86:39–42
- Anantha B, Merugu L, Rao PVDS (2017) A novel single feed frequency and polarization reconfigurable microstrip patch antenna. *AEU Int J Electro Commun* 72:8–16
- Naderi M, Zarrabi FB, Jafari FS, Ebrahimi S (2018) Fractal EBG structure for shielding and reducing the mutual coupling in microstrip patch antenna array. *AEU Int J Electron Commun* 93:261–267
- Bharathi A, Lakshminarayana M, Rao PVDS (2017) A quad-polarization and frequency reconfigurable square ring slot loaded microstrip patch antenna for WLAN applications. *AEU Int J Electro Commun* 78:15–23
- Sethi KK, Rath S, Tripathy SK, Panigrahi M (2015) Application of a stochastic approach in the design of a rectangular microstrip patch antenna. *Procedia Comput Sci* 48:776–780
- Rezvani M, Mohammadi P (2018) Microstrip antenna with aperture reflector and C-shaped dipoles for LTE and wireless communications. *AEU Int J Electron Commun* 94:12–18
- Verma S, Ansari JA (2015) Analysis of U-slot loaded truncated corner rectangular microstrip patch antenna for broadband operation. *AEU Int J Electron Commun* 69(10):1483–1488
- Daliri A, Galehdar A, John S, Wang CH, Ghorbani K (2012) Wireless strain measurement using circular microstrip patch antennas. *Sens Actuators A* 184:86–92
- Sivia JS, Pharwaha AP, Kamal TS (2016) Neurocomputational models for parameter estimation of circular microstrip patch antennas. *Procedia Comput Sci* 85:393–400
- Rashed ANZ, Sharshar HA (2013) Optical microstrip patch antennas design and analysis. *Optik* 124(20):4331–4335
- Nejati A, Sadeghzadeh RA, Geran F (2014) Effect of photonic crystal and frequency selective surface implementation on gain enhancement in the microstrip patch antenna at terahertz frequency. *Phys B Condens Matter* 449:113–120
- Kumar M, Nath V (2016) Analysis of low mutual coupling compact multi-band microstrip patch antenna and its array using defected ground structure. *Eng Sci Technol Int J* 19(2):866–874
- Marotkar DS, Zade P (2016) Bandwidth enhancement of microstrip patch antenna using defected ground structure. In: *International conference on electrical, electronics, and optimization techniques (ICEEOT)*, Chennai, pp 1712–1716. <https://doi.org/10.1109/iceeot.2016.7754978>
- Shareef SKM, Rao RS (2018) Optimal reactive power dispatch under unbalanced conditions using hybrid swarm intelligence. *Comput Electr Eng* 69:183–193
- Boothalingam R (2018) Optimization using lion algorithm: a biological inspiration from lion's social behavior. *Evol Intell* 11:31–52
- Marotkar DS, Zade P, Kapur V (2015) Design of microstrip patch antenna with asymmetric sai shape DGS for Bandwidth enhancement. In: *Applied Electromagnetics conference (AEMC)*, IEEE, pp 1–2
- Kiran MS, Fındık O (2015) A directed artificial bee colony algorithm. *Appl Soft Comput* 26:454–462
- McCall J (2005) Genetic algorithms for modelling and optimisation. *J Comput Appl Math* 184(1):205–222
- Fister I, Fister I Jr, Yang XS, Brest J (2013) A comprehensive review of firefly algorithms. *Swarm Evol Comput* 13:34–46
- Zhang J, Xia P (2017) An improved PSO algorithm for parameter identification of nonlinear dynamic hysteretic models. *J Sound Vib* 389:153–167
- Mirjalili S, Mirjalili SM, Lewis A (2014) Grey wolf optimizer. *Adv Eng Softw* 69:46–61
- Guttula R, Nandavanam VR (2019) Patch antenna design optimization using opposition based grey wolf optimizer. In *communication*

Publisher's Note Springer Nature remains neutral with regard to jurisdictional claims in published maps and institutional affiliations.